

# Steady drainage in emulsions: corrections for surface Plateau borders and a model for high aqueous volume fraction

N. Péron,\* S.J. Cox† S. Hutzler‡ D. Weaire

School of Physics, Trinity College Dublin, Ireland

May 18, 2007

## Abstract

We compare extensive experimental results for the gravity-driven steady drainage of oil-in-water emulsions with two theoretical predictions, both based on the assumption of Poiseuille flow. The first is from standard foam drainage theory, applicable at low aqueous volume fractions, for which a correction is derived to account for the effect of the confinement of the foam. The second arises from considering the permeability of a model porous medium consisting of solid sphere packings, applicable at higher aqueous volume fractions. We find excellent quantitative agreement between experiment and the two theories in each of these limits, providing a master curve for the permeability of foams and emulsions. Using our experimental data, we also demonstrate the analogy between the problem of electrical flow and liquid flow through foams and emulsions.

## 1 Introduction

The general problem of the motion of dispersed particles relative to a continuous fluid phase in response to gravity is composed of two specific situations. The first, *sedimentation* (or “creaming” in the case of emulsions), is the settling of isolated particles, be they solid, liquid (drops) or gas (small bubbles). Sedimentation/creaming tends to bring the particles into contact. The second, known as *drainage* when applied to foams [1], is the flow of the continuous phase around the particles and takes place after sedimentation, when the volume fraction of the continuous phase  $\phi$  is less than a close-packing value of the order of 0.36. As well as being separated in time, the two phenomena are subject to different theories, although they have some features in common.

Solid particles, and even sufficiently small drops of liquid or bubbles, are not compressed enough by gravitational sedimentation to make the drainage process of interest. Emulsions, including those used in applications, are often made with small drops (typically below 100  $\mu$  m [2, 3]

---

\*Present address: Laboratory of Interfaces and Nanosized Systems, Institute of Chemistry, Eötvös Loránd University, 1117 Budapest, Pázmány Péter Sétány 1/A, Hungary

†Present address: Institute of Mathematical and Physical Sciences, University of Wales Aberystwyth, Ceredigion SY23 3BZ, UK

‡corresponding author, email: stefan.hutzler@tcd.ie

if not submicrometric [4, 5]) and the majority of work on the settling of emulsions (called creaming in this context) pertains only to sedimentation; indeed, the volume fraction of the continuous phase is usually above 0.25 and more often above the close-packing limit [6]. We recently began a study of emulsions with drops of a few millimeters in diameter, and values of  $\phi$  down to about 0.1 [7], where drainage *is* important, and we continue that work here.

Drainage theories [8, 9] describe the spatial and temporal variation of the local volume fraction  $\phi$  and the flow rate  $Q$  of the continuous phase for values of  $\phi \lesssim 0.05$  (the *dry* limit). These theories are realized as partial differential equations known as foam drainage equations, derived on the basis of flow through the network of narrow channels, known as Plateau borders. Their predictions are particularly simple if one can restrict oneself to computing the variation of liquid fraction with height. This applies to foams/emulsions confined in narrow cylinders where one finds a uniform volume fraction in any cross-section. In this paper, we address the steady regime in such an experiment, i.e., as continuous phase is added at a constant flow rate  $Q$ , what is the steady state relationship between  $Q$  and  $\phi$ ?

For emulsions, it can be arranged that the viscosity of the continuous phase is small compared to that of the dispersed phase. The dispersed drops are then expected to behave like solid objects and drainage should then proceed in the form of a Poiseuille flow through the Plateau borders, with the velocity of the continuous phase imposed to be zero at the interfaces between the two phases (no-slip boundary condition) [7]. This simple condition on the viscosities is not generally met for aqueous foams (it is inverted and the dispersed phase is less viscous), although experimental observations indicate that a Poiseuille-type flow can be closely approached for particular types of surfactant solutions with rigid air-water interfaces [10]. It follows that drainage in emulsions, besides being of interest in its own right, can provide a benchmark in the limit of Poiseuille drainage for foams. Here the “rigid-interfaces” drainage theory [8] provides quantitative predictions against which experiments on foam drainage can be judged.

An additional feature makes emulsions valuable model systems for studying drainage. We observed that no convective instability occurs up to values of  $\phi$  exceeding 0.42 [7]. Thus steady drainage can be studied far above the value allowed for foams where convective rolls on the scale of the container are triggered above liquid volume fractions  $\phi$  of around 0.15 [11, 12].

In this paper we report experiments of steady drainage in oil-in-water emulsions in vertical glass cylinders. The volume fraction  $\phi$  is varied between about 0.02 and 0.45, bridging the, usually separated, domains of sedimentation and drainage. The viscosity of the oil that constitutes the dispersed phase is a factor of 350 larger than that of the water that makes up the continuous phase. We undertake a full quantitative comparison (including prefactors) of the experimental data for  $\phi$  as a function of  $Q$  with two *ab initio* theories: (i) the drainage theory initially developed for low liquid fraction drainage in foam, and (ii) the permeability of a model porous medium consisting of spheres, at higher water volume fraction. A new correction is introduced in the drainage theory to account for the walls of the cylinder. Finally we present our case for a generalised conductance, covering both the flow of liquid and electrical current through foams and emulsions.

The following section presents the experimental method. The experimental results are in section 3. In section 4 we compare the experimental results to calculations from foam drainage theory. This theory is refined to account for finite size effects due to the walls of the confining

cylinder. In section 5, the experimental results are compared to calculations of the permeability of sphere packings and in section 6 to the electrical conductivity of foams and emulsions. Section 7 presents the conclusions.

## 2 Methodology and experimental set-up

The aim of our *forced drainage* experiments is to determine the volume fraction of an oil-in-water emulsion, stabilised by adding commercial washing-up liquid to the water, as a function of the drainage flow rate at steady state. The set-up is shown in Fig. 1. The vertical glass cylinder of diameter  $D$  containing the emulsion is connected via tubing and rubber plugs to a communicating vessel (e.g. a 1 litre phial) whose height and water level can be adjusted to externally tune the height of the air-water interface in the cylinder. Prior to the measurements, monodisperse oil drops are injected at a constant rate by a pipette at the bottom of the cylinder and their number  $n$  is recorded. Buoyancy gathers the drops into an emulsion.

The draining aqueous solution is fed back into the emulsion by adding solution to the top at a constant flow rate  $Q$ . Our flow rate supplying device was either a glass burette or a syringe pump (Infors, Basel, Switzerland) equipped with a 100 cm<sup>3</sup> glass syringe. This device allows us to accurately set constant flow rates as low as 0.0001 cm<sup>3</sup>/s. We used silicone oil (Dow Corning 200/350 cS Fluid, BDH Silicon product). The density at 25°C, given by the manufacturer, is  $\rho_o = 0.968 \text{ g/cm}^3$  and the coefficient of thermal expansion is 0.00096 °C<sup>-1</sup>; the viscosity is around  $\eta_o = 3.5 \text{ g cm}^{-1} \text{ s}^{-1}$ . The aqueous solution was made up of de-ionised water with 1% v/v of commercial dish-washing liquid as the surfactant.

In order to vary the density difference, some of the experiments were performed using mixtures of de-ionised water and analytical grade ethanol for the continuous phase. The ethanol concentration was restricted to be not more than 15% v/v for reasons of stability: beyond this concentration, coalescence events (neighbouring drops merging with one another) occurred before the measurements could be completed. Many studies in the literature address specifically the coalescence that proceeds concurrently with, or subsequent to, creaming [13, 14, 15, 16]. The measurements reported in the present paper concern creaming with no coalescence. The absence of any coalescence event could be verified visually as the drops were macroscopic and remained monodisperse. All experiments were conducted at ambient temperature. The water/ethanol mixtures were prepared at least 12 hours in advance and all dishes and liquids were left in the room overnight prior to the experiments.

For such a set-up it is experimentally observed (and predicted by the foam drainage equation [17]) that the aqueous volume fraction in a foam or emulsion under steady drainage is a uniform function of height except near the bottom boundary where the aqueous solution meets the emulsion. In the following we refer to the aqueous volume fraction  $\phi$  as the constant value away from the lower boundary.

In the limit as the flow rate  $Q$  tends to zero, for the case of Poiseuille flow as in our emulsions,  $\phi$  scales as:

$$\phi = c_\phi \sqrt{Q}, \quad (1)$$

where  $c_\phi$  is a constant that is dependent on the experimental parameters. The aim of our work is firstly to determine this constant experimentally, and secondly to compare it to theoretical predictions.

This requires an accurate experimental determination of  $\phi$ . To do this we first measure the total length of the emulsion in the cylinder,  $L(Q)$ , using a ruler once the steady regime (i.e. a constant value of  $L(Q)$ ) is reached. We then rinse the emulsion with water devoid of surfactant to merge the oil drops in the cylinder into a single homogeneous phase of oil. We denote by  $L_0$  the length of this column of oil. Then

$$\phi = \frac{L(Q) - L_0 - \Delta L(Q)}{L(Q)} \quad (2)$$

where  $\Delta L(Q)$  is an additional length associated with the excess water at the bottom boundary, where the drops become spherical, derived explicitly in Appendix A.

The additional length  $\Delta L(Q)$  is maximal at  $Q = 0$  and decreases with  $Q$ , as the value of  $\phi$  increases. For  $Q = 0$ , it is of the order  $l_0^2/b$  [1], where  $b$  is the equivalent sphere diameter of the oil drops and  $l_0$  is the capillary length,

$$l_0 = \sqrt{\gamma/\Delta\rho g}. \quad (3)$$

Here  $\gamma$  is the interfacial tension,  $\Delta\rho$  is the difference in density between the two phases and  $g$  is the acceleration due to gravity. In the experiments described here,  $\gamma \approx 10$  mN/m [18]. For large values of  $\phi$  or long columns of foam,  $\Delta L(Q)$  can be neglected, as described in Appendix A. The expression for  $\phi$  then reduces to

$$\phi \simeq 1 - \frac{L_0}{L(Q)}. \quad (4)$$

In one case (data in Fig. 2), water remained trapped in the oil, making the determination of  $L_0$  an inaccurate procedure. Instead, the value of  $L(0)$  was obtained using the following extrapolation procedure, and used in Eq. 4 in place of  $L_0$ . Combining Eqs. 1 and 4 we obtain

$$Q = c_\phi^{-2} \left( \frac{L(Q) - L(0)}{L(Q)} \right)^2. \quad (5)$$

We fitted this expression to the experimental data on successive ranges of flow rate  $[0, Q_{up}]$  with decreasing values of the upper limit  $Q_{up}$ . The fit parameters  $L(0)$  and  $c_{\phi,exp}$  were then observed to tend monotonically towards a well-defined limit at low flow rate. The experimental data and the related limiting fitting curve are shown in Fig. 2, where the fit parameter  $L(0)$  is marked by a cross. The fit is good on a restricted range of  $L(Q) - L(0)$  corresponding to  $\phi \lesssim 0.06$ , while deviations occur for larger values of  $L(Q) - L(0)$ .

To compare with theory we also need to know the diameter of the equal-size oil drops. Since we release the drops one-by-one into the column, it is easy to count their total number  $n$ . The equivalent sphere diameter of the oil drops  $b$  is then given by

$$b = \left( \frac{3L_0 D^2}{2n} \right)^{1/3}. \quad (6)$$

Overall, the reported experiments cover the range  $0.00015 \text{ cm}^3 < Q < 0.16 \text{ cm}^3$  in flow rate,  $0.025 < \phi < 0.45$  in aqueous volume fraction and  $9.0 \text{ mm} < D < 12.4 \text{ mm}$  in cylinder diameter.

The value of the drop diameter  $b$  is always close to 3 mm; so the cylinder diameter is not very large compared to the drop size.

### 3 Experimental results

Our steady-state data for the variation of aqueous volume fraction with  $Q$  is summarised in Fig. 3. In Fig. 3a we plot data for emulsions in cylinders of differing diameters  $D$  but almost identical drop diameter  $b$  in all the measurements. We can see that as the cylinder diameter is increased, a given value of  $\phi$  is only sustained with a larger value of  $Q$ .

Fig. 3b shows data for varying density difference  $\Delta\rho = \rho_w - \rho_o$ , where  $\rho_w$  is the density of the ethanol/water mixture. As shown in Table 1,  $\Delta\rho$  decreases and the viscosity  $\eta_w$  increases as a function of the ethanol concentration. (Density-matching, where  $\Delta\rho = 0$ , is reached at an ethanol concentration of about 22% v/v ; earlier work based on the density-matching between oil and mixtures of water and alcohol is found in the book by Plateau [20]). Measurements were carried out with the same emulsion successively subjected to drainage by each of the ethanol-water mixtures listed in Table 1, in increasing order of concentration. The four sets of data in Fig. 3b confirm that any given value of  $\phi$  requires a greater flow rate when the density contrast is larger.

Results in the low flow-rate limit are compared with predictions of the foam drainage theory in the following section. In section 5 we calculate the *reduced permeability* of the emulsions as a function of  $\phi$  from the flow rate measurements, and we will compare them to theoretical predictions of permeabilities from the literature.

### 4 Low aqueous volume fractions

In the theory for Poiseuille drainage in a bulk foam,  $\phi^2$  is proportional to  $Q$  in the limit of small  $\phi$ , see Eq. 1. This proportionality is experimentally confirmed, as shown in Fig. 4, and holds approximately for  $\phi$  up to 0.06, corresponding to  $Q = 0.0011\text{cm}^3/\text{s}$  in our experiment. As shown in Fig. 5a, the drops are observed to approach a polyhedral geometry with straight edges under these low drainage flow rates. (Fig. 2 of Ref. [7] also shows the Plateau borders of emulsions at low water volume fraction.) In addition, the emulsion in Fig. 5a presents an ordered structure with spatial periodicity along the axis of the cylinder. This extends the sequence of ordered cylindrical emulsions described previously [7]. Our experiments confirm that for values of the ratio of cylinder to drop diameter,  $\lambda \equiv D/b$ , significantly above unity, the arrangement of monodisperse drops into an ordered structure is generally fortuitous and the structure obtained is often disordered.

The geometrical properties (e.g. edge-length and surface area per unit volume) of any packing of monodisperse cells are quantitatively well represented by a periodic packing of “Kelvin” tetrakaidecahedra [21], shown in Fig. 6a. This Kelvin packing is also the most tractable theoretical model for a 3D foam, so we choose to compare our experimental data to the classical theory for drainage in Kelvin foam.

Assuming a bulk foam consisting of space-filling Kelvin cells (Fig. 6a), the theoretical value

for the coefficient  $c_\phi$  is given by [1, eq. 11.26]

$$c_{\phi,th}^2 = 5.35 \frac{3\chi_{pb}\eta_w}{\Delta\rho g} V_b^{-2/3} A_{cyl}^{-1}. \quad (7)$$

Here  $V_b$  is the bubble volume,  $A_{cyl}$  the cross-sectional area of the cylinder and  $\chi_{pb} \approx 49.8$  a dimensionless factor, calculated numerically, that characterizes the particular shape of the cross-section of a Plateau border. Other packings of monodisperse bubbles, ordered or random, result in deviations of the prefactor 5.35 by less than 2% [8, 21].

For our experimental parameters we compute  $c_{\phi,th}^2 = 5.77 \text{ s cm}^{-3}$  while a fit to the data results in  $c_{\phi,exp}^2 = 3.37 \text{ s cm}^{-3}$  (the slope of the continuous line in Fig. 4). The prediction of  $c_\phi$  is nearly twice the value that fits the experimental data and we therefore have a quantitative disagreement between experiment and theory that is not due to the assumption of a particular bulk structure.

In view of the relatively small value of the ratio of cylinder diameter to drop diameter,  $\lambda \equiv D/b \approx 2.78$ , finite size effects due to the walls should be anticipated. As a refinement to the existing theory, the drops from the peripheral layer of the emulsion may be treated distinctly from those of the bulk. In the idealized Kelvin structure, the surface drops consist of two halves equal in volume but different in geometry, as shown in Fig. 6b: one fits to the bulk Kelvin structure while the other rests against the wall. The surface cells are arranged into a hexagonal structure as described in [1, §13]. The volume  $V_b$  of a Kelvin cell can be written as

$$V_b = 2^{7/2} r^3 \quad (8)$$

where  $r$  is an edge length (all edges have equal length). This volume is also equal to  $(\pi/6)b^3$ , hence

$$r = \frac{\pi^{1/3}}{3^{1/3} 2^{3/2}} b. \quad (9)$$

If the curvature of the glass wall is neglected, then the thickness of the surface layer of half-Kelvin cells is  $r$  and the surface area  $s$  that each of them occupies on the wall is given by

$$s = 2^{5/2} r^2. \quad (10)$$

This area is also given by  $s = (3^{3/2}/2)w^2$  where  $w$  is the length of one edge of the surface hexagonal cells. It follows that

$$w = \frac{2^{7/4}}{3^{3/4}} r. \quad (11)$$

The interior of the cylinder may be split into a central region of diameter  $D - 2r$ , treated by the existing bulk drainage model, and a surface region of thickness  $r$  consisting of the half surface hexagonal cells (Fig. 6c). The draining fluid is found in a network of channels of two types: (i) the bulk Plateau borders of cross-section  $A_{pb} = c_{pb}\delta^2$  where  $c_{pb} = \sqrt{3} - \pi/2$  and  $\delta$  is the radius of curvature of the water/oil interfaces; (ii) the surface Plateau borders of cross-section  $A_{spb} = c_{spb}\delta^2$  where  $c_{spb} = 2 - \pi/2$ . With these assumptions, and using the above expressions for  $r$ ,  $s$  and  $w$ , we find that, to second order in  $\delta/b$ , the total volume fraction of the aqueous phase in the system is

$$\phi = (1 + a_1 \lambda^{-1} a_2 \lambda^{-2}) \frac{2^{3/2} 3^{5/3}}{\pi^{2/3}} c_{pb} \frac{\delta^2}{b^2}. \quad (12)$$

where

$$a_1 = \left( \frac{2^{11/4} c_{spb}}{3^{3/4} c_{pb}} - \frac{8}{3} \right) \frac{\pi^{1/3}}{3^{1/3} 2^{3/2}} \approx 1.8627 \quad (13)$$

and

$$a_2 = - \left( \frac{2^{11/4} c_{spb}}{3^{3/4} c_{pb}} - \frac{8}{3} \right) \frac{\pi^{2/3}}{3^{2/3} 2^3} \approx -0.6688 \quad (14)$$

The total flow rate  $Q$  is the sum of the flow rates in the bulk region and on the surface:

$$Q = Q_{bulk} + Q_{surf}. \quad (15)$$

The surface and the bulk region are assumed to be connected together only through horizontal Plateau borders; these are not accounted for in the flow rates. The bulk contribution is given by [1]:

$$Q_{bulk} = \sigma_s^f \Delta \rho g \frac{\pi}{4} (D - 2r)^2. \quad (16)$$

Here  $\sigma_s^f$  is the flow conductivity:

$$\sigma_s^f = \frac{1}{3} l_v \frac{A_{pb}^2}{\eta_w \chi_{pb}} \quad (17)$$

where  $l_v$  is the length of bulk Plateau border per unit volume:

$$l_v = \frac{12}{2^{7/6}} \frac{1}{V_b^{2/3}}. \quad (18)$$

Only the surface Plateau borders need to be accounted for in the calculation of  $Q_{surf}$ . The calculation of the flow rate in the two-dimensional network of surface Plateau borders is analogous to the previous calculation in three dimensions:

$$Q_{surf} = \sigma_{s,s}^f \Delta \rho g \pi D. \quad (19)$$

In this expression,  $\sigma_{s,s}^f$  is the surface flow conductivity:

$$\sigma_{s,s}^f = \frac{1}{2} l_s \frac{A_{spb}^2}{\eta_w \chi_{spb}} \quad (20)$$

where  $\chi_{spb}$  is the dimensionless coefficient calculated numerically for surface Plateau borders,  $\chi_{spb} \approx 50.7$  [22]. The factor of 1/2 accounts for the random orientation in two dimensions of the surface channels. The variable  $l_s$  is the length of surface Plateau borders per unit surface, therefore  $l_s = 3w/s$ .

Summing the two contributions to  $Q$ , we obtain

$$Q = (1 + c_1 \lambda^{-1} + c_2 \lambda^{-2}) \frac{3^{2/3} \pi^{1/3}}{2^{1/2}} \frac{c_{pb}^2}{\chi_{pb}} \frac{\Delta \rho g}{\eta_w} D^2 b^2 \frac{\delta^4}{b^4} \quad (21)$$

where

$$c_1 = \left( \frac{2^{1/4} \pi^{1/3}}{3^{1/12}} \left( \frac{c_{spb}^2}{c_{pb}^2} \frac{\chi_{pb}}{\chi_{spb}} \right) - \frac{2^{1/2} \pi^{1/3}}{3^{1/3}} \right) \approx 9.6234 \quad (22)$$

and

$$c_2 = \frac{\pi^{2/3}}{2 \times 3^{2/3}} \approx 0.5156. \quad (23)$$

Now, the ratio  $\delta/b$  can be eliminated between Eq. 12 and Eq. 21. We find the following expression for  $\phi^2$  as a function of  $Q$ :

$$\phi^2 = f(\lambda) \frac{2^{3/2} 3^{8/3}}{\pi^{2/3}} \chi_{pb} \frac{Q}{Q_0}. \quad (24)$$

Here  $Q_0$  is a characteristic flow rate defined by

$$Q_0 \equiv \frac{\pi}{4} \frac{\Delta \rho g}{\eta_w} D^2 b^2 \quad (25)$$

and  $f(\lambda)$  is the fraction

$$f(\lambda) = \frac{(1 + a_1 \lambda^{-1} + a_2 \lambda^{-2})^2}{1 + c_1 \lambda^{-1} + c_2 \lambda^{-2}}. \quad (26)$$

So that the cylinder is large enough to allow drops to form in the bulk,  $\lambda$  must exceed a value of about 1.6, corresponding to  $f(\lambda) > 0.5$  [23]. Fig. 7 shows that  $f$  increases as a function of  $\lambda$  and reaches unity as  $\lambda$  approaches infinity. In this limit, where the wall effects are expected to be negligible, it can be shown that Eq. 24 is equivalent to Eq. 1 with  $c_\phi$  given by Eq. 7.

For the measurements plotted in Fig. 4 we have  $\lambda = 2.78$ , therefore  $f(\lambda) \approx 0.554$ . We thus calculate that the wall effects approximately double the flow rate. As previously estimated [24], calculated, and verified by sophisticated experiments [25, 26], each of the surface Plateau borders carries a much larger flow rate than a bulk Plateau border. We calculate here that for the same longitudinal pressure gradient, the ratio between the flow rate through a surface Plateau border and through a bulk Plateau border is  $(c_{spb}^2/c_{pb}^2)(\chi_{pb}/\chi_{spb}) \approx 7.0$ . The coefficient  $c_{\phi,th}^2$  is now 3.20 s/cm<sup>3</sup>, in close agreement with the experimental value 3.37 s/cm<sup>3</sup>. Also, the resulting expression  $\phi^2 = c_{\phi,th}^2 Q$ , plotted as a dashed line in Fig. 4, is very close to the experimental data.

Therefore, in a regime of low liquid fraction, the drainage theory is successful in quantitatively predicting the dependence of aqueous volume fraction  $\phi$  on flow rate  $Q$  provided that wall effects are included. This justifies *a posteriori* the statement in the introduction that drainage in emulsions (with low viscosity ratio  $\eta_w/\eta_o \approx 1/350$  of water to oil phase) is of Poiseuille type.

## 5 Analysis for high aqueous volume fraction

Figure 8 is a plot of  $\ln(Q/Q_0)$  as a function of  $\phi$  for all our experimental data, taken for a variety of cylinder diameters and viscosities;  $Q_0$  is the characteristic flow rate defined in Eq. 25. The collapse of the data onto a single master curve confirms that given the aqueous volume fraction  $\phi$ , which acts as a geometrical parameter, the value of  $Q$  for steady drainage does scale with respect to the experimental parameters according to the characteristic flow rate  $Q_0$  of Eq. 25. Our system

has the diameter ratio  $\lambda$  as an additional geometrical parameter that quantifies the wall effects. From the observed collapse of our data, the variations of  $\lambda$  in the explored range ( $2.65 < \lambda < 3.68$ ) are of limited impact. The prediction for small aqueous volume fraction (Eq. 24) with  $\lambda = 2.78$  is plotted with a continuous line. As already observed in section 4 this calculation is in agreement with the experimental points for  $0 < \phi < 0.06$ , but not far beyond this range.

At larger aqueous volume fractions, as already stated in the context of foams or emulsions [9, 27, 28], drainage may be treated identically to flow at low Reynolds numbers in porous media by the classical Darcy equation:

$$Q = \frac{k}{\eta_w} A |\vec{\nabla \Pi}|, \quad (27)$$

where  $A$  is the cross-section through which the flow proceeds,  $|\vec{\nabla \Pi}|$  is the gradient of driving pressure and  $k$  is the permeability of the medium. The equivalent of our variable  $\phi$  in the context of porous media is called the porosity [29]. The relation between  $k$  and  $\phi$  depends on the geometry of the continuous phase or porous network. The cross-section  $A$  in our experiments is  $A = (\pi/4)D^2$ . Neglecting the impact on  $|\vec{\nabla \Pi}|$  of finite size effects due to the cylinder wall, we have  $|\vec{\nabla \Pi}| = (1 - \phi) \Delta \rho g$ , resulting in:

$$\frac{Q}{Q_0} = (1 - \phi) \frac{k}{b^2}. \quad (28)$$

The permeability of spatially-periodic packings of overlapping spheres to Stokes flow is given by [30]:

$$\frac{k}{d^2} = \frac{1}{K} \frac{V_0}{6\pi a d^2}, \quad (29)$$

where  $d$  is the centre-to-centre distance between closest-neighbour spheres,  $K$  is the coefficient of friction (numerical values are given in Tab. 3 of ref. [30]),  $a$  is the radius of the spheres and  $V_0$  is the volume of a unit cell of the packing. We have:

$$V_0 = \beta d^3, \quad (30)$$

where  $\beta$  is a coefficient depending on the structure of the periodic packing (BCC structure:  $\beta = 4/3^{3/2}$ ; FCC structure:  $\beta = 2^{-1/2}$ ). It follows that the reduced flow rate  $Q/Q_0$  can be expressed as:

$$\frac{Q}{Q_0} = (1 - \phi)^{1/3} \frac{\beta^{1/3}}{6^{5/3} \pi^{1/3}} \frac{1}{\left(\frac{a}{d}\right) K}. \quad (31)$$

where we have used  $(\pi/6)b^3 = (1 - \phi)V_0$ .

The ratio  $a/d$  can be calculated for all values of  $\phi$  as detailed in Appendix B. The reduced flow rate  $Q/Q_0$  can thus be calculated as a function of  $\phi$  by Eq. 31 using this  $a/d$  value and the value of  $K$  found in Table 3 of Ref. [30]. The resulting plots of  $\ln(Q/Q_0)$  assuming a BCC or an FCC structure are shown in Fig. 8, together with the experimental data. We find that the BCC calculation (dotted line) is in good agreement with the experimental data for  $\phi > 0.1$ , i.e. where the prediction for small aqueous volume fraction (continuous line) starts to deviate significantly.

As shown in Fig. 5b for  $\phi = 0.16$ , and for larger values of  $\phi$  in Ref. [7], the shape of the oil drops in these conditions becomes spherical, just as they are in the model of Ref. [30]. However, our emulsions were, in general, structurally disordered and no estimation could be made concerning whether the structure is close to a BCC or other ordered structure. As for the small flow rate theory (section 4), assuming some type of ordered structure allows a tractable theoretical approach.

The theoretical reduced flow rate assuming an FCC structure (Fig. 8) is smaller than the BCC reduced flow rate in the whole range covered by  $\phi$ . The FCC model is in particular discrepancy with the experimental points for small values of  $\phi$ . This observation is consistent with independent experiments on static aqueous foams where the structure is BCC in a range of small values of  $\phi$  and switches to FCC for  $\phi > 0.2$  [31].

The sphere packing models have a fundamental inadequacy at describing drainage in emulsions (or in foams) at small values of  $\phi$ . Approaching the dry limit, the geometries of the continuous phase networks in the sphere packings (with curvature radius  $a$ ) differ increasingly from the network of Plateau borders of foams and emulsions. For a finite value of  $\phi$  larger than zero (BCC:  $\phi \cong 0.005501$ ; FCC:  $\phi \cong 0.035897$ ) strictly no flow is allowed through the packing. This explains the increasing deviation of the theoretical prediction with respect to the experimental data in the dry limit.

## 6 Generalised conductivity: the analogy between liquid and electrical flow

In the limit in which the volume fraction of the continuous phase tends to zero, liquid flow and electrical conductivity through foams and emulsions are in some sense equivalent [1]. Here, we use our data to show that the analogy between these two quantities actually holds for a wide range of  $\phi$ . Since existing drainage theory is only valid in the low  $\phi$  limit, the correspondence demonstrated below should provide guidance for the development of a generalised theory of drainage, valid for arbitrary  $\phi$ .

The relative electrical conductivity  $\sigma^e$  of a foam or emulsion is defined by  $\sigma^e = \sigma_s^e / \sigma_c^e$  where  $\sigma_c^e$  and  $\sigma_s^e$  are the electrical conductivity of the continuous phase and the entire sample, respectively. Feitosa *et al.* [32] recently published the following empirical formula for the variation of  $\sigma^e$  with the volume fraction  $\phi$  of the continuous phase, based in part upon a large amount of historical data:

$$\sigma^e = 2\phi(1 + 12\phi)/(6 + 29\phi - 9\phi^2) \quad (32)$$

Lemlich's [33] expression for the relative *flow* conductivity  $\sigma^f$ , defined in a similar way and valid in the limit as  $\phi \rightarrow 0$ , is:

$$\sigma^f = \phi/3$$

Note that Eq. 32 contains this limit.

To derive an effective *flow* conductivity for a foam or emulsion, we proceed from Eq. 16, which makes no assumptions about  $\phi$  (cf. Eq. 17, which does). Neglecting the influence of surface flow,

the flow conductivity of the entire sample is given by

$$\sigma_s^f = \frac{Q}{\Delta \rho g A_{cyl}}. \quad (33)$$

We may define an *effective flow conductivity* for flow through a *single* Plateau border as

$$\sigma_c^f = \frac{A_{pb}}{\eta_w \chi_{pb}}. \quad (34)$$

The relative flow conductivity is then:

$$\sigma^f = \frac{\sigma_s^f}{\sigma_c^f} = \frac{Q}{Q_0} \chi_{pb} \left( \frac{6}{\pi} \right)^{2/3} \frac{V_b^{2/3}}{A_{pb}}. \quad (35)$$

Both  $V_b$  (from Eq. 18) and  $A_{pb}$  are related to the length of the Plateau border network per unit volume  $l_v$ , which enables us to express  $\sigma^f$  in terms of  $\phi = l_v A_{pb}$ . For a Kelvin packing this results in

$$\sigma^f = \frac{12}{27/6} \left( \frac{6}{\pi} \right)^{2/3} \chi_{pb} \frac{Q}{Q_0} \phi^{-1} = 8.23 \chi_{pb} \frac{Q}{Q_0} \phi^{-1}. \quad (36)$$

Note that if we were to write  $Q$  in terms of  $\phi$  using the appropriate expression (Eq. 7) for Poiseuille drainage, and valid for low values of  $\phi$ , then the above equation reduces to Lemlich's expression.

In Fig. 9 we have evaluated Eq. 36 for our emulsion drainage data and show it as a function of  $\phi$ . The equivalence of relative flow conductivity and electrical conductivity, with the latter given by Eq. 32, is convincingly demonstrated, for values of  $\phi$  up to 0.2.

This requires several comments. In deriving Eq. 36 we have taken for  $l_v$  (length of Plateau borders per unit volume) the value for Kelvin packing. This is known to be a good approximation for random monodisperse packings [21] at low  $\phi$ . Our data seems to suggest that its range of validity extends even up to  $\phi \simeq 0.2$ . It may be speculated that knowledge of  $l_v$  for larger values of  $\phi$  could increase this range even further.

Values of  $\chi_{pb}$  different from 49.8 could be used when Poiseuille flow is not appropriate. [DRENCKHAN REF?]

Surface Plateau borders, which needed to be included when relating the predictions of Poiseuille flow drainage theory to our data, were not taken into account. They could be incorporated in the above theory of flow conductance, but it appears that their effect is very limited in this particular representation of the data.

Finally, we have not plotted the high  $\phi$  data for the emulsions containing ethanol since this data shows more experimental scatter than the data for non-ethanol based emulsions.

In summary, we believe that the merit of Fig. 9 lies in summarising two different transport problems in one graph. Since the electrical conductivity data is highly reliable at this stage, this can give information about the drainage behaviour of emulsions/foams for values of liquid fraction that are difficult to access experimentally.

## 7 Conclusion

The experimental results for drainage of an emulsion were quantitatively compared with two theories in which the flow of the continuous phase is of the Poiseuille type, i.e. with zero velocity at the interface of the two liquids. In the limit of low aqueous volume fraction, we predict that wall effects can result in a substantial positive correction to the flow rate (estimated to be a multiplying factor  $1/f(\lambda)$ ). With this refinement, the foam drainage theory provides a good quantitative prediction of the relation between  $Q$  and  $\phi$ . Our results suggest a limit of validity of the low volume fraction drainage regime around  $\phi = 0.06$ . For higher aqueous volume fraction, analogies to the flow through porous media prove very useful. In particular, measurement of the reduced permeability allows for a collapse of a wide variety of drainage data. We find a surprising agreement with calculations for a model porous medium with a BCC arrangement of spherical pores. Further investigation is required and should focus on the treatment of wall effects in this theory.

The problem of liquid flow in foams or emulsions is closely linked to the problem of electrical conductivity in such materials and a generalised conductivity can be identified that solves both transport problems. Its usefulness in deriving a generalised flow equation needs to be explored in future work.

## 8 Acknowledgements

This research was supported by the European Space Agency (14914/02/NL/SH, 14308/00/NL/SG) (AO-99-031) CCN 002 MAP Project AO-99-075) and Science Foundation Ireland (RFP 05/RFP/PHY0016). SJC acknowledges support from EPSRC (EP/D071127/1).

## A Profile of aqueous volume fraction at the lower boundary of the emulsion

The foam drainage equation, once integrated, gives an equation for the profile of aqueous volume fraction  $\varphi(z)$  in steady drainage (Eq. 8 of Ref. [17]):

$$\frac{z}{l_1} = \frac{1}{2\phi^{1/2}} \left[ \left( \arctan \frac{\varphi(0)^{1/2}}{\phi^{1/2}} - \operatorname{arccoth} \frac{\varphi(0)^{1/2}}{\phi^{1/2}} \right) - \left( \arctan \frac{\varphi(z)^{1/2}}{\phi^{1/2}} - \operatorname{arccoth} \frac{\varphi(z)^{1/2}}{\phi^{1/2}} \right) \right]. \quad (37)$$

Here  $z$  is the vertical coordinate measured upwards from the lower boundary of the emulsion. The variable  $l_1$  in Eq. 37 is a characteristic length, defined by

$$l_1 \equiv 2\sqrt{\tilde{c}} \frac{l_0^2}{b} \quad (38)$$

where  $b$  is the diameter of the bubbles or drops,  $\tilde{c}$  is a constant with value close to 0.333 in the case of a foam with a Kelvin structure [1] and  $l_0$  is the capillary length as in Eq. 3. As above,  $\phi$  is the bulk water volume fraction i.e. the limit which  $\varphi(z)$  reaches as  $z \rightarrow \infty$ .

Here the origin  $z = 0$  corresponds to the bottom of the emulsion, where the drops take the shape of spheres. Therefore our value of  $\varphi(0)$  is that of the void volume fraction for close-packed spheres,  $\varphi(0) = 0.36$ .

Our aim is to compute the height  $L$  of the emulsion in the general case. Accounting for the amounts of oil and of water in the system, we have:

$$L = L_0 + \int_0^L \varphi(z) dz \quad (39)$$

where  $L_0$  is the length of the column of oil when the emulsion has fully collapsed. The integral on the right hand side of Eq. 39 can be transformed using integration by parts:

$$\int_0^L \varphi(z) dz = L \varphi(L) - \int_{\varphi(0)}^{\varphi(L)} z d\varphi(z). \quad (40)$$

The length  $L$  may thus be split into three contributions:

$$L = L_0 + \phi L + \Delta L \quad (41)$$

where the sum  $L_0 + \phi L$  is the length calculated from Eq. 39 by setting  $\varphi(z)$  equal to the bulk value  $\phi$  everywhere, and letting  $\Delta L$  account for the contribution of the bottom boundary effects to the total column length. (Note that this is the equation used for the definition of aqueous volume fraction  $\phi$  in Eq. 2.) Using Eqs. 41, 39, 40 and Eq. 37, the following expression can be obtained for  $\Delta L$ :

$$\Delta L = \phi^{1/2} l_1 \left[ \left( \frac{\varphi(0)^{1/2}}{\phi^{1/2}} - \arctan \frac{\varphi(0)^{1/2}}{\phi^{1/2}} \right) - \left( \frac{\varphi(L)^{1/2}}{\phi^{1/2}} - \arctan \frac{\varphi(L)^{1/2}}{\phi^{1/2}} \right) \right]. \quad (42)$$

When  $L$  is large compared to  $l_1$ , the volume fraction at the top approaches its asymptotic value i.e.  $\varphi(L) \approx \phi$ . In this limit Eq. 42 reduces to

$$\Delta L = \phi^{1/2} l_1 \left[ \frac{\varphi(0)^{1/2}}{\phi^{1/2}} - \arctan \frac{\varphi(0)^{1/2}}{\phi^{1/2}} - 1 + \frac{\pi}{4} \right], \quad (43)$$

shown in Fig. 10.

For our study of dry emulsions with only water as the continuous phase, shown in Fig. 2, the value of  $L(0)$  is 66.7cm, over 50 times greater than the corresponding value of  $\Delta L(0)$ , which we consequently neglected ( $\Delta L(0)$  is calculated to be  $\varphi(0)^{1/2} l_1$  from Eq. 43 in the limit  $\phi \rightarrow 0$ , equivalent to  $Q \rightarrow 0$ ).

Values of aqueous volume fraction  $\phi$  in the shorter columns ( $L_0 = 20.45\text{cm}$  and  $13.06\text{cm}$ ) exceeded 0.1, therefore from Eq. 43 with  $\varphi(0) = 0.36$  we have  $\Delta L < 0.188 l_1 < 0.26 \text{ cm}$ . It follows that the use of Eq. 4 is justified. This also holds for the emulsions with water and 15% v/v of ethanol as the continuous phase which had aqueous volume fractions higher than 0.2, since in this case  $\Delta L < 0.088 l_1 < 0.4 \text{ cm}$ .

## B Calculation of the ratio $a/d$

Due to the overlap between neighbours in the sphere packings, the relation between the ratio  $a/d$  and  $\phi$  depends on the value of  $\phi$ . We have in the BCC case:

$$\begin{aligned} 1 - \frac{3^{1/2} \pi}{8} < \phi < 1 & : \quad \phi = 1 - 3^{1/2} \pi \left( \frac{a}{d} \right)^3 \\ 1 - \left( \frac{3^{3/2}}{4} - 1 \right) \pi < \phi < 1 - \frac{3^{1/2} \pi}{8} & : \quad \phi = 1 - 3^{1/2} \pi \left[ 3 \left( \frac{a}{d} \right)^2 - 3 \left( \frac{a}{d} \right)^3 - \frac{1}{4} \right] \\ 0.005501... < \phi < 1 - \left( \frac{3^{3/2}}{4} - 1 \right) \pi & : \quad \phi = 1 - 3^{1/2} \pi \left[ \left( 3 + \frac{3^{3/2}}{2} \right) \left( \frac{a}{d} \right)^2 - 6 \left( \frac{a}{d} \right)^3 - \frac{1}{4} - \frac{1}{2 \times 3^{1/2}} \right] \end{aligned} \quad (44)$$

and in the FCC case:

$$\begin{aligned} 1 - \frac{\pi}{2^{1/2} \times 3} < \phi < 1 & : \quad \phi = 1 - \frac{2^{5/2} \pi}{3} \left( \frac{a}{d} \right)^3 \\ 1 - 2^{1/2} \pi \left( \frac{3}{2} - \frac{20}{3^{5/2}} \right) < \phi < 1 - \frac{\pi}{2^{1/2} \times 3} & : \quad \phi = 1 - 2^{1/2} \pi \left( 6 \left( \frac{a}{d} \right)^2 - \frac{20}{3} \left( \frac{a}{d} \right)^3 - \frac{1}{2} \right). \end{aligned} \quad (45)$$

Given a value of  $\phi$ , the value of  $a/d$  can be calculated by solving Eq. 44 or Eq. 45, possibly numerically, for instance with a Newton algorithm.

## References

- [1] D. Weaire, S. Hutzler, 1999 *The Physics of Foams* (Oxford: Oxford University Press).
- [2] E. Dickinson, C. Ritzoulis, J. Colloid Interface Sci. **224**, 148 (2000).
- [3] S. Kumar, T. W. Pirog, D. Ramkrishna, Chem. Eng. Sci. **55**, 1893 (2000).
- [4] D.M. Mueth, J.C. Crocker, S.E. Esipov, D. Grier, Phys. Rev. Lett. **77**, 578 (1996).
- [5] R. Chanamai, D.J. McClements, Colloids Surf. A **172**, 79 (2000).
- [6] A. Kumar, S. Hartland, Can. J. Chem. Eng. **63**, 368 (1985).
- [7] S. Hutzler, N. Péron, D. Weaire, W. Drenckhan, Eur. Phys. J. E **14**, 381 (2004).
- [8] D. Weaire, S. Hutzler, G. Verbist and E.A.J.F. Peters, “A review of foam drainage” Advances in Chemical Physics **102**, 315 (1997).
- [9] S.A. Koehler, S. Hilgenfeldt, and H.A. Stone, Langmuir **16**, 6327 (2000).
- [10] A. Saint-Jalmes, Y. Zhang and D. Langevin, Eur. Phys. J. E **15**, 53 (2004).
- [11] S. Hutzler, D. Weaire, R. Crawford, Europhys. Lett. **41** 461 (1998).

- [12] M.U. Vera, A. Saint-Jalmes, D.J. Durian, Phys. Rev. Lett. **84**, 3001 (2000).
- [13] A.A.K. Jeelani, R. Hosig, E.J. Windhab AIChE J. **51**, 149 (2005).
- [14] S.R. Reddy, H.S. Fogler, J. Colloid Interface Sci. **82**, 128 (1981).
- [15] H. Wang, R.H. Davis, J. Fluid Mech. **295**, 247 (1995).
- [16] H. Wang, R.H. Davis, J. Colloid Interface Sci. **181** 93 (1996).
- [17] Verbist G., Weaire D. and Kraynik A. M., J. Phys.: Condens. Matter **8**, 3715 (1996).
- [18] J. Bibette, J. Colloid Interface Sci. **147**, 474 (1991).
- [19] *CRC Handbook of Chemistry and Physics, 70th Ed.*, 1989, Ed. R. C. Weast (CRC, Florida).
- [20] J. A. F. Plateau, 1873, *Statique expérimentale et théorique des liquides soumis aux seules forces moléculaires*, 1st vol. (Gauthier-Villars, Paris).
- [21] A.M. Kraynik, D.A. Reinelt and F. van Swol, Phys. Rev. E **67**, 031403 (2003).
- [22] L. Alonso, G. Bradley, S.J. Cox, S. Hutzler, 2002 “Flow through borders and vertices in foam drainage”, poster presented at Eufoams 2002, Manchester, UK.
- [23] N. Pittet, N. Rivier and D. Weaire, Forma **10**, 65 (1995).
- [24] A.V. Pertsov, S.E. Botchenkov, S.V. Drozhzhin, E.V. Porodenko, Colloid J. **63**, p. 213 (2001).
- [25] S.A. Koehler, S. Hilgenfeldt, E.R. Weeks, H.A. Stone, Phys. Rev. E **66**, 040601(R) (2002).
- [26] S.A. Koehler, S. Hilgenfeldt, E.R. Weeks, H.A. Stone, J. Colloid Interface Sci. **276**, p. 439 (2004).
- [27] J.D. Sherwood, G.H. Meeten, C.A. Farrow, N.J. Alderman, J. Chem. Soc. Faraday Trans. **87** 611 (1991).
- [28] J.D. Sherwood, Chem. Eng. Sci. **48**, 3355 (1993).
- [29] E. Guyon, J.-P. Hulin, L. Petit, 1991 *Hydrodynamique Physique* (Interéditions/Editions du CNRS, Paris).
- [30] R.E. Larson and J.J.L. Higdon, Phys. Fluids A **1**, 38 (1989).
- [31] A. van der Net, W. Drenckhan, D. Weaire, S. Hutzler, Soft Matter **2**, 129 (2006).
- [32] K. Feitosa, S. Marze, A. Saint-Jalmes, D.J. Durian, 2005 “Electrical conductivity of dispersions: from dry foams to dilute suspensions” J. Phys.: Condens. Matter **17**, 6301-5.
- [33] R. Lemlich, J. Colloid Interface Sci. **64** 107-110 (1978)

Concentration in ethanol % v/v	Density difference $\Delta\rho$ g/cm <sup>3</sup>	Viscosity $\eta_w$ g cm <sup>-1</sup> s <sup>-1</sup>
0	0.0256	1.002 10 <sup>-2</sup>
5	0.0184	1.183 10 <sup>-2</sup>
10	0.0121	1.386 10 <sup>-2</sup>
15	0.0065	1.633 10 <sup>-2</sup>

Table 1: Properties of water and ethanol mixtures. The density difference is calculated by  $\Delta\rho = \rho_w - \rho_o$  where  $\rho_w$  is the density of the mixture of water and ethanol [19];  $\eta_w$  is the viscosity of the mixture of water and ethanol [19].

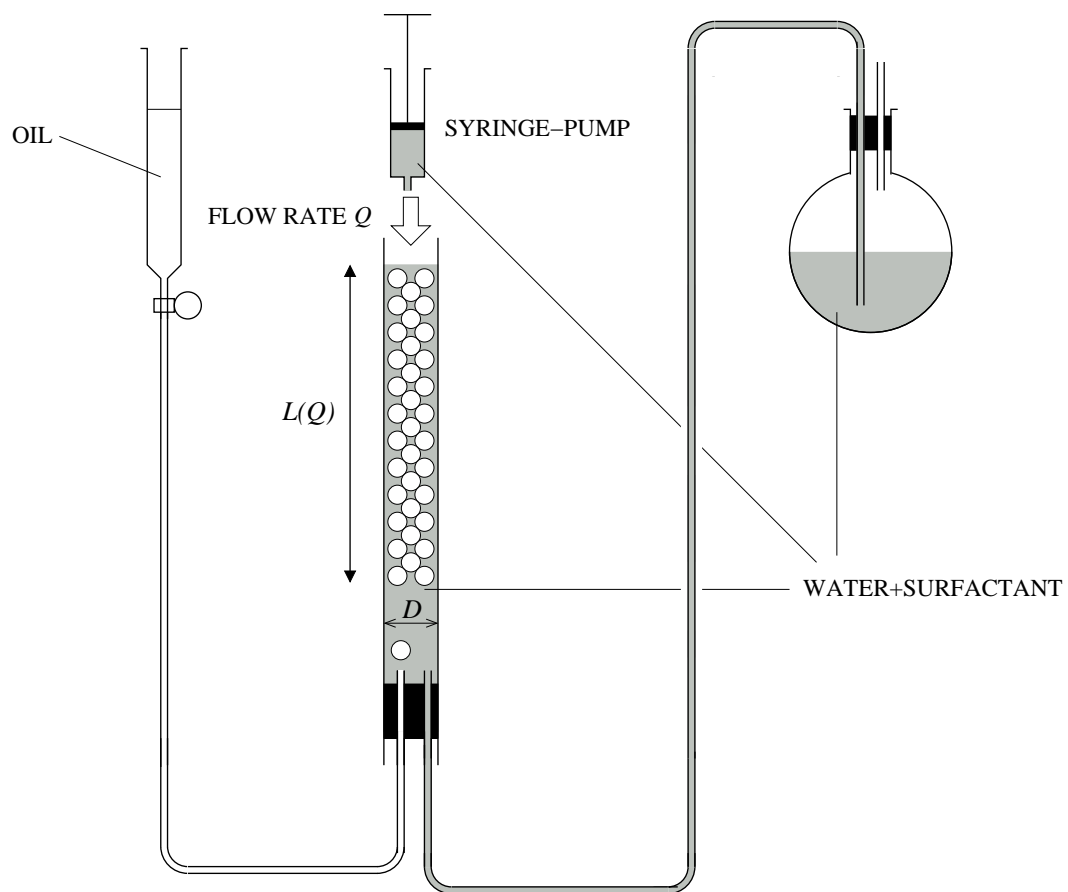


Figure 1: Experimental set-up for the study of steady drainage in an emulsion. The syringe pump provides a constant input of aqueous surfactant solution at a flow rate  $Q$ .

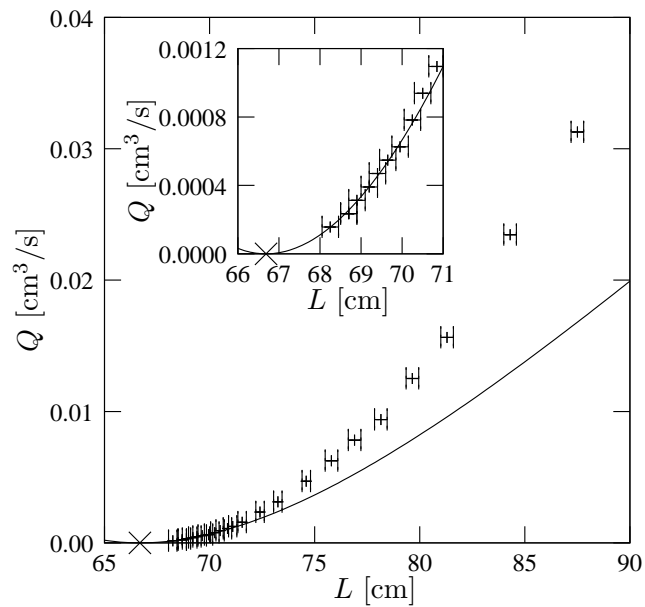


Figure 2: Emulsion length  $L$  versus flow rate  $Q$  as the dry limit is approached. Since the drops did not coalesce at the end of the experiment, the extrapolation procedure described in the text was used to find a value of  $L(0) = 66.68\text{cm}$  (marked by  $\times$  on the abscissa). The cylinder diameter was  $D = 9.0\text{ mm}$  and the drop diameter  $b = 3.23\text{ mm}$ . The continuous line is the corresponding quadratic fit. The insert is a zoom on small values of  $Q$ .

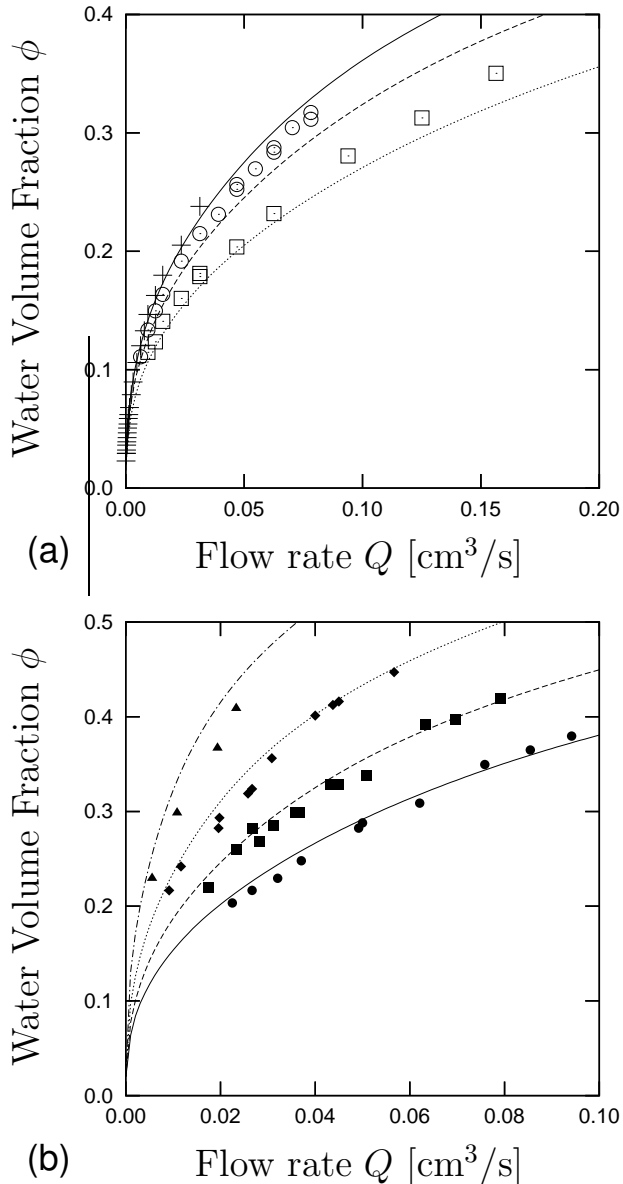


Figure 3: Water volume fraction as a function of the flow rate. (a) Measurements with cylinders of different diameters, without ethanol. Data marked +:  $D = 9.0$  mm,  $L(0) = 66.68$  cm,  $b = 3.23$  mm (as in Fig. 2). Data marked ⊙:  $D = 9.9$  mm,  $L_0 = 20.45$  cm,  $b = 3.37$  mm. Data marked □:  $D = 12.4$  mm,  $L_0 = 13.06$  cm,  $b = 3.37$  mm. The lines are derived from the theory of high liquid volume fraction, as presented in section 5 (calculated from Eq. 31 for a BCC structure and values of  $Q_0$  calculated from Eq. 25). (b) Measurements for one emulsion subjected successively to drainage with an increasing concentration of ethanol in water: ●: 0% v/v; ■: 5% v/v; ♦: 10% v/v; ▲: 15% v/v.

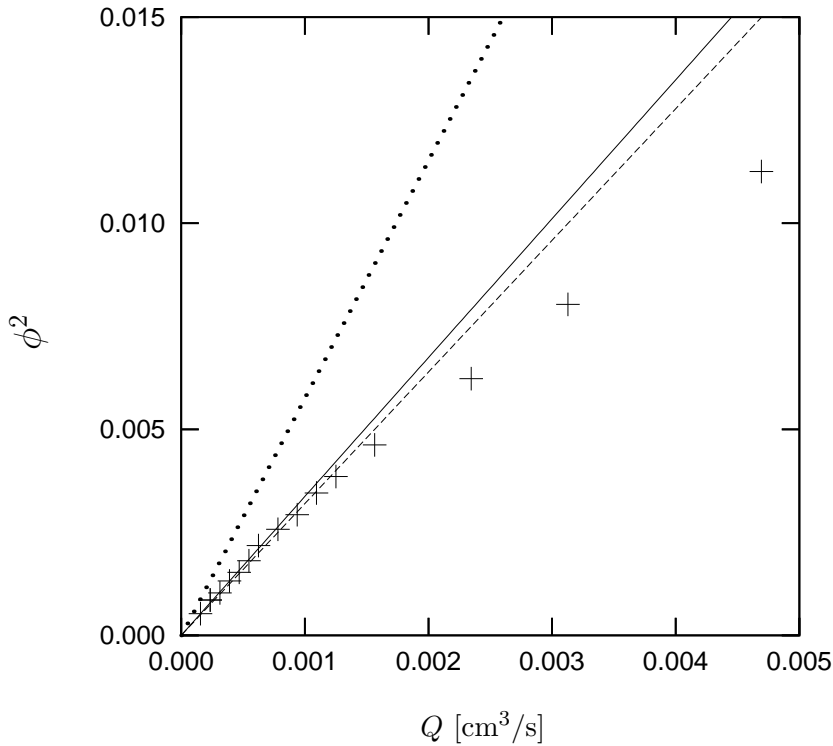


Figure 4: Squared water volume fraction as a function of flow rate for the data of Fig. 2 (+). The continuous line is the linear fit in the limit as  $Q$  tends to zero:  $\phi^2 = c_{\phi,exp}^2 Q$  with  $c_{\phi,exp}^2 = 3.37$  s/cm<sup>3</sup>. The dotted line is the prediction of standard drainage theory and the dashed line is the prediction when the Plateau borders along the walls are taken into account, see Eq. 24, with  $\lambda = 2.78$  in these experiments.

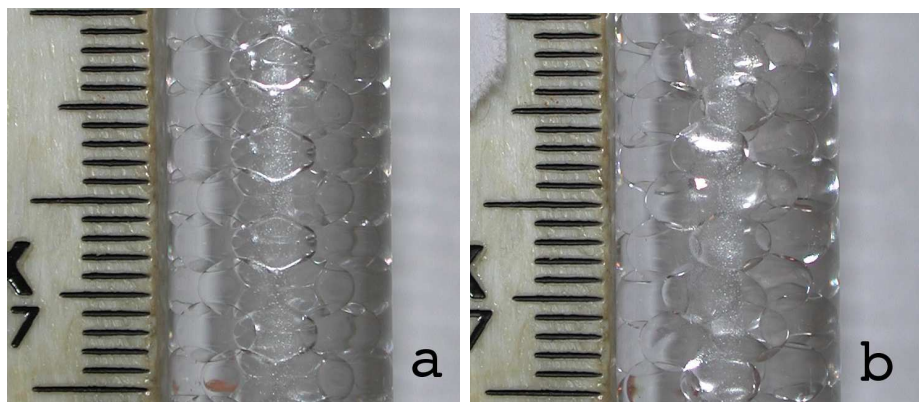


Figure 5: Side view of emulsion under drainage, for: a)  $Q = 0.00031$  cm<sup>3</sup>/s and  $\phi \approx 0.032$ ; b)  $Q = 0.0125$  cm<sup>3</sup>/s and  $\phi \approx 0.16$ . The internal diameter of the glass cylinder is 9 mm.

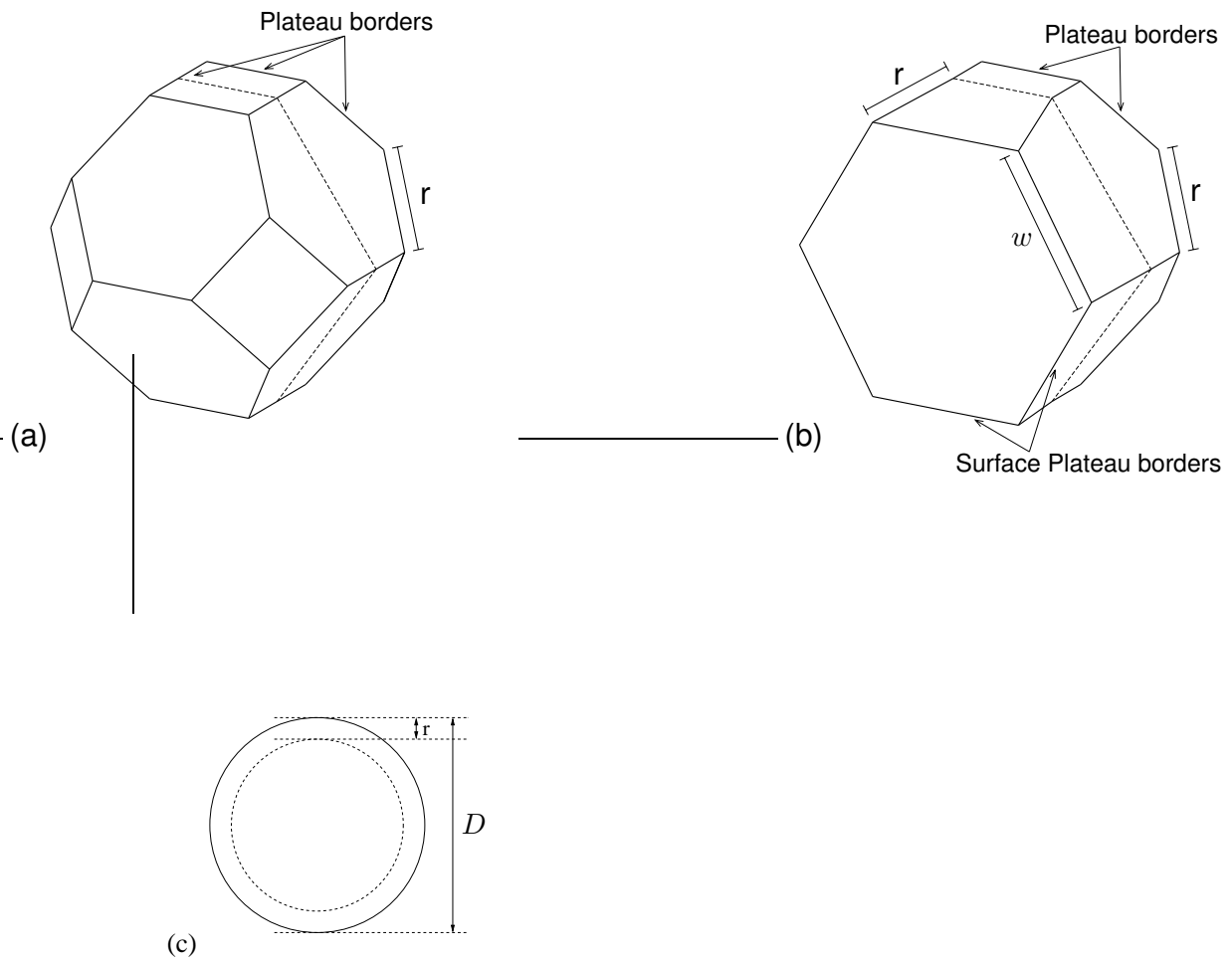


Figure 6: Geometry of bulk and surface Kelvin cells, used for numerical calculations of drainage which include surface flow. (a) bulk Kelvin cell of edge length  $r$ ; (b) surface Kelvin cell split (dashed line) into bulk and surface halves; (c) cross-section showing the bulk region and the surface region of the interior of the cylinder.

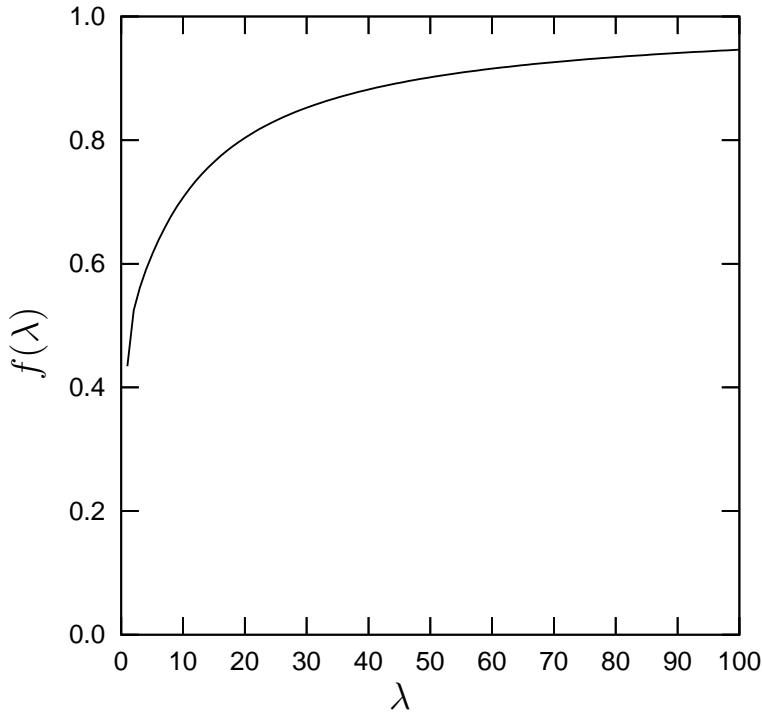


Figure 7: The function  $f(\lambda)$  is a numerical correction factor which takes account of flow along the wall of the container. Here  $\lambda$  is the ratio of cylinder diameter to drop diameter. (Note that foam structures with bulk Plateau borders require  $\lambda > 1.6$ .)

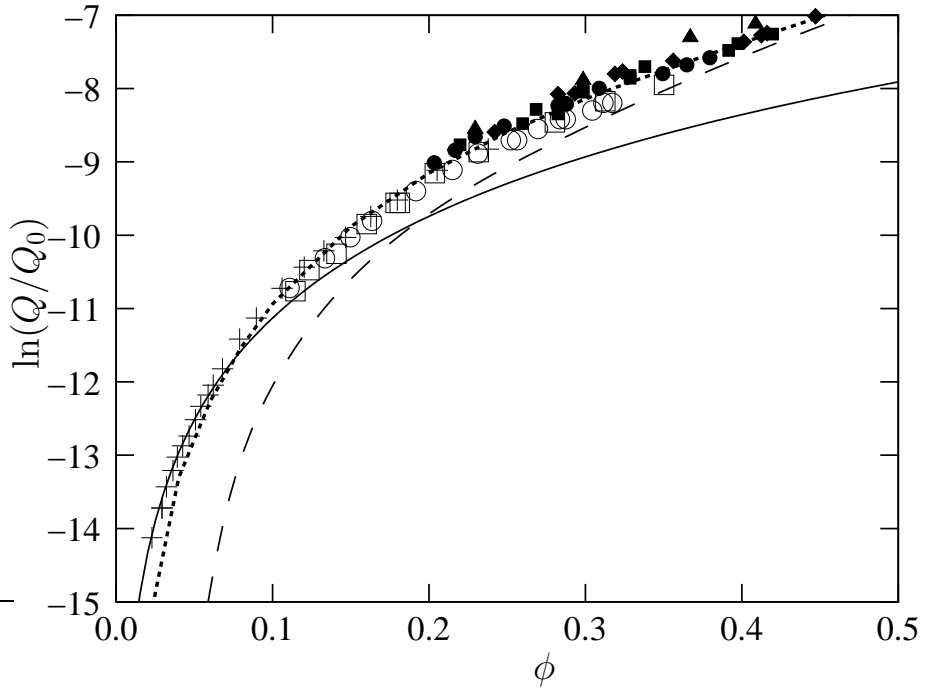


Figure 8: Logarithm of the reduced flow rate  $Q/Q_0$  as a function of the aqueous volume fraction  $\phi$ . Data points are the experimental data of Fig. 3 (same symbols). Continuous line: the dry-limit prediction obtained by inverting Eq. 24 with  $\lambda = 2.78$ . Dotted line: model of Eq. 31 assuming a BCC structure. Dashed line: model of Eq. 31 assuming an FCC structure.

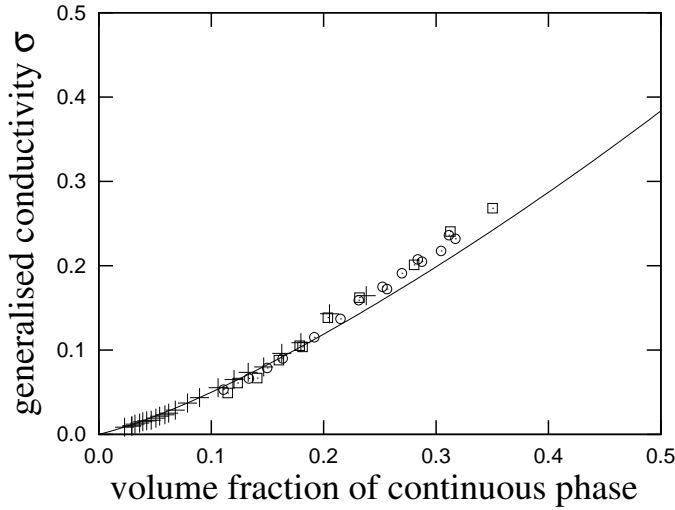


Figure 9: Generalised conductivity as a function of the volume fraction  $\phi$  of continuous phase. Data points are from our drainage experiments on emulsions (Figure 3a) converted into flow conductivities  $\sigma^f$  using Eq. 36. The solid line is an empirical function (Eq. 32) describing the relative electrical conductance of foams. The good agreement demonstrates the analogy between the problem of electrical flow and liquid flow through foams and emulsions.

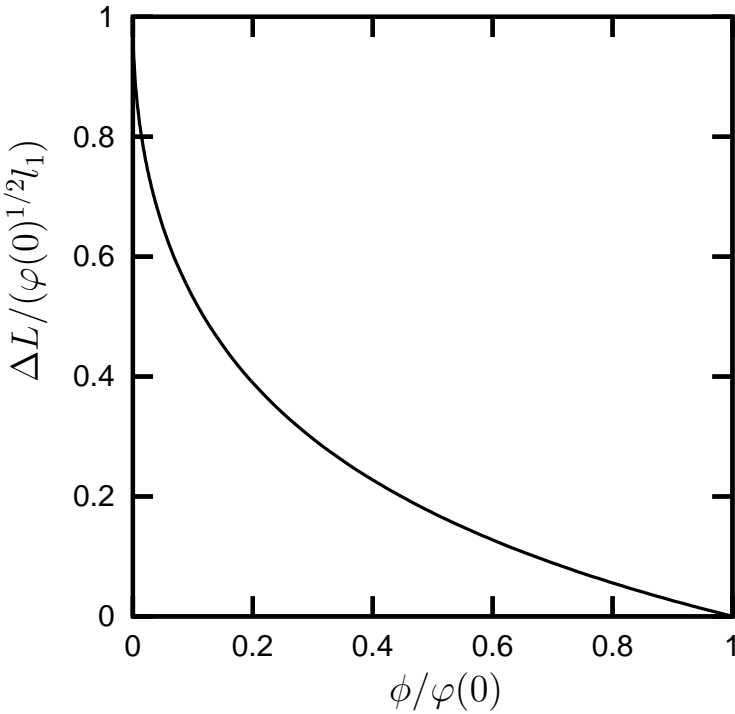


Figure 10: Normalized excess length of an emulsion or foam column as a function of the (normalized) bulk liquid fraction. This length, which is calculated from Eq. 43, is due to capillary effects at the bottom of the emulsion.